Available online at www.sciencedirect.com
SCIENCE DIRECT®
International Journal of Mass Spectrometry 232 (2004) 17–24
International Journal of Mass Spectrometry
www.elsevier.com/locate/ijms

Theoretical characterizations of novel $C_2H_5O^+$ reactions

Charles E. Hudson, David J. McAdoo*

Marine Biomedical Institute, University of Texas Medical Branch, 301 University Boulevard, Galveston, TX 77555-1069, USA

Received 25 September 2003; accepted 5 November 2003

Abstract

Assorted reactions of $C_2H_5O^+$ isomers are characterized by theory, including tracing their courses by means of intrinsic reaction coordinate computations. We establish that $CH_3CH{=}OH^+$ eliminates methane by transferring H from oxygen to a methyl hydrogen and then to the CC bond to produce $CHO^+ + CH_4$. This adds to the limited knowledge of the involvement of hypervalent structures in the reactions of cations in the gas phase. Second, we characterized the course of $CH_3CH{=}OH^+ \rightarrow H_3O^+ + HC{\equiv}CH$. In this dissociation, H first migrates from the methyl to the oxygen to give O-protonated vinyl alcohol, a stable intermediate. Then the H_2O swings outward to over the middle of the CC bond while one of the two hydrogens on the non-O-bearing carbon revolves to between the oxygen and the two carbons, leading to formation of a $[H_3O^+\,HC{\equiv}CH]$ complex. This complex contains sufficient energy to dissociate its partners because a high barrier is crossed in its formation. Third, we found that methane elimination from $CH_3O^+{=}CH_2$ involves stretching of the CH_3–O bond and then rotation of the methyl so that a methyl hydrogen is pointed directly toward the oxygen. This reaction is completed by further rotation of the methyl to abstract a methylene hydrogen to the opposite side of the methyl from that initially bonded to oxygen. This clearly establishes that this dissociation takes place through an ion–neutral complex. Each of the reaction coordinates for the three preceding reactions traverses a novel bonding stage involving H, evidence that such are not unusual in gas phase ion chemistry. Finally, we showed that in the rearrangement $CH_3O^+{=}CH_2 \rightarrow CH_2{=}O^+CH_3$, before H_t is transferred CH_2 rotates around the C=C bond from being in the skeletal plane to being perpendicular to it, and H_t remains in the skeletal plane throughout its transfer. This pathway appears to balance avoiding an orbital symmetry-forbidden suprafacial transition state with minimizing the strain that would be present in an antarafacial transition state for a 1,3-H-shift.

Keywords: Ab initio; $C_2H_5O^+$; Elimination reactions; Ion–neutral complexes; Hypervalent ions; Intrinsic reaction coordinates

1. Introduction

The isomerizations and dissociations of $C_2H_5O^+$ isomers are of long-standing interest in gas phase ion chemistry [1–3]; even so, they still have unusual and incompletely understood features. For example, in methane elimination from $CH_3CH{=}OH^+$ (**1**), H migrates from O to the CC bond through a hypervalent stage by way of a methyl H [4]. However, this trajectory has not been fully described. Hypervalent entities may be common but little recognized in unimolecular gas phase ion chemistry. It is also not certain whether methane elimination from $CH_3O^+{=}CH_2$ (**2**) is ion–neutral complex-mediated [3] or not, making **1** and **2** together a useful model for exploring what determines the type of pathway an elimination takes. Therefore, we here characterize methane eliminations from $C_2H_5O^+$ isomers at higher levels of theory than accomplished previously and by intrinsic reaction coordinate calculations (IRC). We also trace the path of **1** $\rightarrow H_3O^+ + HC{\equiv}CH$. Despite much experimental study, this reaction is not fully understood, and to our knowledge it has not hitherto been described by theory. This reaction involves a novel simultaneous migration of a hydrogen and H_2O. Finally, we determine whether the degenerate isomerization $CH_3O^+{=}CH_2$(**2**) $\rightarrow CH_2{=}O^+CH_3$(**2′**) is antarafacial, which would conserve orbital symmetry, suprafacial, possibly violating conservation of orbital symmetry [5], or in between. All of these are pathways known to occur in 1,3-H-transfers in ions in the gas phase [6,7]. Previous theoretical studies showed that at the halfway point in **2** $\rightarrow$ **2′** the migrating H is midway between the carbons in the skeletal plane and each CH_2 is bisected by that plane [8,9], consistent with reaction by the third possible pathway.

* Corresponding author. Tel.: +1-409-772-2939; fax: +1-409-762-9382.
E-mail address: djmcadoo@utmb.edu (D.J. McAdoo).

1387-3806/$ – see front matter © 2003 Elsevier B.V. All rights reserved.
doi:10.1016/j.ijms.2003.11.001

Table 1
Energies for $CH_3CH{=}OH^+ \rightarrow HCO^+ + CH_4$ and $CH_3CH{=}OH^+ \rightarrow H_3O^+ + HC{\equiv}CH$

	B3LYP/6-31G(d)[a]	B3LYP/6-311+G(d,p)[b]	QCISD/6-311G(d,p)[c]	QCISD(T)/6-311G(2df,p)[c]	ZPE
$CH_3CH{=}OH^+$ (**1t**)	−154.136706	−154.186802	−153.779357	−153.872570	176.8
$CH_3CH{=}OH^+$ (**1c**)	−154.136033	−154.185821	−153.778532	−153.871786	177.1
TS(**1t** → **1c**)	−154.100523	−154.152487	−153.738745	−153.834221	167.2
TS(**1c** − CH_4)	−154.022641	−154.077260	−153.668618	−153.766083	157.4
HCO^+	−113.545291	−113.581797	−113.321057	−113.385130	42.6
CH_4	−40.518389	−40.533933	−40.401643	−40.425593	116.4
$HCO^+ + CH_4$	−154.063680	−154.115730	−153.722700	−153.810723	159.0
$CH_2{=}CH{-}OH_2^+$ (**3**)	−154.090736	−154.147900	−153.740974	−153.835158	174.9
TS(**1t** → **3**)	−154.015982	−154.073907	−153.659065	−153.758473	156.7
H_3O^+	−76.689085	−76.731072	−76.557913	−76.596595	88.3
$HC{\equiv}CH$	−77.325646	−77.356646	−77.126990	−77.180451	68.6
$H_3O^+ + HC{\equiv}CH$	−154.018652	−154.087718	−153.684903	−153.777046	157.1
[$HC{\equiv}CH$ H_3O^+] (**4**)	−154.051068	−154.120091	−153.713597	−153.807931	159.2
TS(**3** → **4**)	−154.032360	−154.098289	−153.686077	−153.780272	153.6
$CH_3CH{=}OH^+$ (**1t**)	0	0	0	0	
$CH_3CH{=}OH^+$ (**1c**)	2	3	2	2	
TS(**1t** → **1c**)	85	81	97	91	
TS(**1** − CH_4)	280	268	271	260	
$HCO^+ + CH_4$[d]	174	169	131	145	
$CH_2{=}CH{-}OH_2^+$ (**3**)	119	102	99	96	
TS(**1** → **3**)	297	276	296	279	
$H_3O^+ + HC{\equiv}CH$	290	240	228	231	
[H_3O^+ $HC{\equiv}CH$] (**4**)	207	158	155	152	
TS(**3** → **4**)	251	209	222	219	

Values in the upper section are in hartrees; corresponding values in the lower section are in kJ mol^{-1}. The latter are all relative to the corresponding energies for **1t**.
[a] At B3LYP/6-31G(d) geometries.
[b] At B3LYP/6-311+G(d,p) geometries.
[c] At QCISD/6-31G(d,p) geometries.
[d] Experimental: 168.1 kJ mol^{-1}.

2. Theory

All calculations were performed using the Gaussian 98W package of programs [10]. Geometries were obtained by B3LYP/6-31G(d) and B3LYP/6-311G+(d,p) hybrid functional theories and QCISD/6-311G(d,p) ab initio theory. Energies were obtained by those and B3LYP/6-311+G(d,p), B3LYP/6-311+G(2df,p), QCISD(T)/6-311G(d,p) and QCISD(T)/6-311G+(2df,p) levels of theory. Stable species at energy minima were identified by having only positive vibrational frequencies, and points with only one imaginary vibrational frequency were considered to be transition states. Reaction pathways were traced by IRC methods [11,12] with a B3LYP/6-31G(d) basis set. Zero point energies were obtained by multiplying those derived from B3LYP/6-31G(d) frequencies by the scaling factor 0.9806 [13]. The three highest levels of theory applied generally gave relative energies consistent within 20 kJ mol^{-1}, and therefore quite satisfactory (Tables 1 and 2). However, when acetylene was involved, B3LYP/6-31G(d) theory gave rel-

Table 2
Energies for $CH_3O^+{=}CH_2 \rightarrow HCO^+ + CH_4$ and $CH_3O^+{=}CH_2 \rightarrow CH_2{=}O^+CH_3$

	B3LYP/6-31G(d)	B3LYP/6-311+G(2df,p)	QCISD/6-311G(d,p)	QCISD(T)/6-311+G(2df,p)	ZPE
$CH_3O^+{=}CH_2$ (**2**)	−154.112474	−154.164579	−153.751737	−153.844775	178.2
TS(**2** − CH_4)	−154.008523	−154.063432	−153.646487	−153.732242	156.3
HCO^+	−113.545291	−113.587861	−113.321057	−113.385130	42.6
CH_4	−40.518389	−40.535248	−40.401643	−40.425593	116.4
$HCO^+ + CH_4$	−154.063680	−154.123109	−153.722687	−153.810723	159.0
2 → **2′**	−154.037712	−154.086034	−153.679167	−153.776652	168.6
$CH_3O^+{=}CH_2$	0	0	0	0	
TS(**2** − CH_4)	251	244	254	228	
$HCO^+ + CH_4$[c]	119	90	67	70	
2 → **2′**	187	197	181	169	

Values in the upper section are in hartrees; corresponding values in the lower section are in kJ mol^{-1}.
(a) At B3LYP/6-31G(d) geometries. (b) At QCISD/6-31G(d,p) geometries (c) Experimental: 94 kJ mol^{-1}.

ative energies differing substantially from those at higher levels of theory, suggesting problem with triple bonds at that level of theory.

3. Results and discussion

3.1. $CH_3CH{=}OH^+$ (1) $\rightarrow HCO^+ + CH_4$

Characterization of the appropriate transition state previously demonstrated that H (H_t) migrates from O to the methyl carbon by way of a hypervalent methyl hydrogen (H_h) during methane elimination from **1** [4], but the reaction coordinate for this pathway has not been traced. Previously, a high energy, hypervalent intermediate was found in this reaction by restricted Hartree-Fock theory, whereas only a transition state was located by MP2 theory [4]. Therefore the reaction coordinate of this interesting reaction was not hitherto fully established. Energies obtained at several levels of theory for stationary points on this pathway are given in Table 1, and the geometries of ground and transition states are given in Fig. 1. We located a transition state but no local minima along this pathway by B3LYP/6-31G(d), B3LYP/6-311+G(d,p) and QCISD/6-31G(d,p) theories (the only theories used to obtain geometries), so it is very unlikely that there is a high energy intermediate in the course of this reaction. Thus, hypervalent configurations arising in the course of gas phase ionic reactions may not generally be stable minima.

As in our previous study in which only stationary points were characterized [4], in results of IRC calculations H_t first migrates from the O to a hydrogen on the methyl (H_h) of **1**, rendering H_h hypervalent. The OH_t, H_tH_h and CH_h distances along this pathway are plotted as a function of the CC distance in Fig. 2. Both H_t and H_h are in the skeletal plane in the ground state of **1** and the H_hCCO dihedral angle is 0°; those atoms remain in this orientation throughout the reaction. In the first stage of the reaction, H_t transfers from the oxygen to H_h to form a hypervalent structure. During this stage, ROH_t (R denotes interatomic distances throughout) increases from 0.980 to 1.780 Å, as RCC increases from 1.453 to 1.554 Å (from **1** to the transition state). These values differ from those in Fig. 1a because the former were obtained by B3LYP/6-31G(d) theory and those in the figure by QCISD/6-31G(d,p) theory. At the same time, RH_tH_h decreases from 2.355 to 0.889 Å. The "corresponding" equilib-

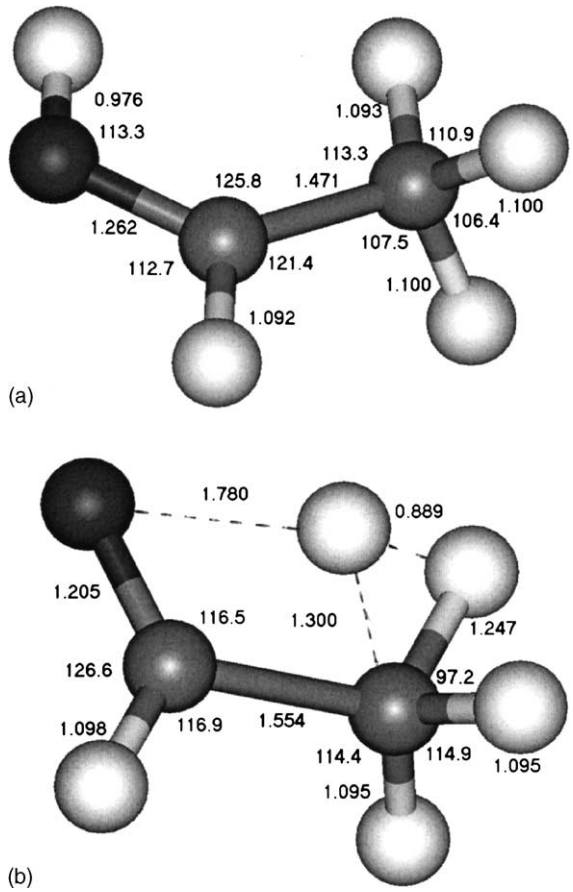

Fig. 1. (a) Geometry of the "cis" (**1c**) form of $CH_3CH{=}OH^+$. All geometries given in this and remaining figures are at the QCISD/6-311G(d,p) level of theory. (b) The geometry of TS(**1c** $\rightarrow HCO^+ + CH_4$). H_t moves from O to a methyl hydrogen (H_h) to the CC bond in this reaction.

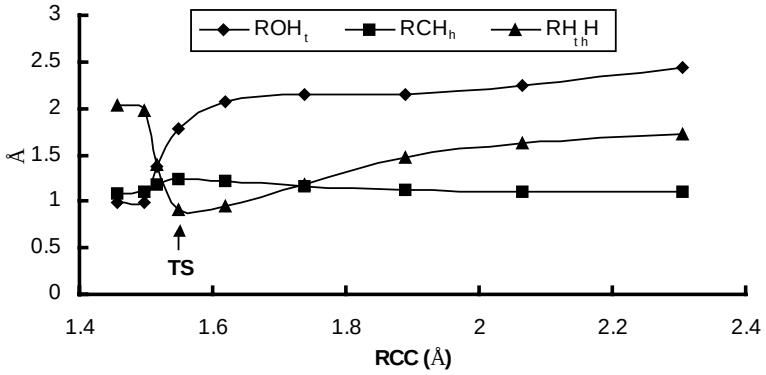

Fig. 2. Changes in the OH_t, CH_h and H_tH_h distances in the course of the methane elimination from **1** ("H_tH_h" occurs in the course of methane elimination from $CH_3CH{=}OH^+$).

rium bond length for H_2 is 0.742 Å (the length of the unperturbed H–H bond in H_2 [14]). Thus, at the transition state, H_t is closely associated with H_h such that an H_2 molecule is almost fully formed when the CC bond is only beginning to lengthen. A similar "H_2" exists in CH_5^+ [15,16]. The H_tH_h "bond" in the reaction coordinate for **1** → **2** is in the same plane as the axis of the CC bond; H_2 elimination from a 1-propyl-like configuration of $C_3H_7^+$ occurs with H_2 similarly aligned to a CC bond [17]. The presence of "H_2" in the preceding systems suggests that it is a favorable motif in closed shell cations. The occurrence of $H_2 \cdots CH_2X^+$ stages along the reaction coordinates for H_2 elimination from CH_3XH^+ (X = NH_2, OH, F, SiH, Cl) support this [18]. Other reactions with hypervalent stages are methane elimination from $C_4H_9^+$ [17] and methane elimination from $C_4H_8^+$ [19]. Thus such stages may not be uncommon in gas phase ion chemistry.

In the second stage of the elimination of methane from **1**, RH_tH_h increases and RH_tC decreases as H_t inserts into the CC bond and CH_4 and HCO^+ separate. Throughout this stage, H_tH_h is above the methyl carbon and stays coplanar with the CC axis. Simultaneously, the other two hydrogens on C2 maintain symmetric locations on opposite sides of the skeletal plane. Thus, the transition state for this reaction contains a pentavalent carbon with bonds to the two hydrogens in "H_2", two normal CH bonds, and a CC bond.

3.2. $CH_3CH{=}OH^+ \rightarrow H_3O^+ + HC{\equiv}CH$

The formation of H_3O^+ from **2** has received considerable experimental attention [1–3], but to our knowledge has not been described by theory. Energies obtained by present work are given in Table 1; structures of intermediates and transition states comprise Fig. 3 and a potential diagram for

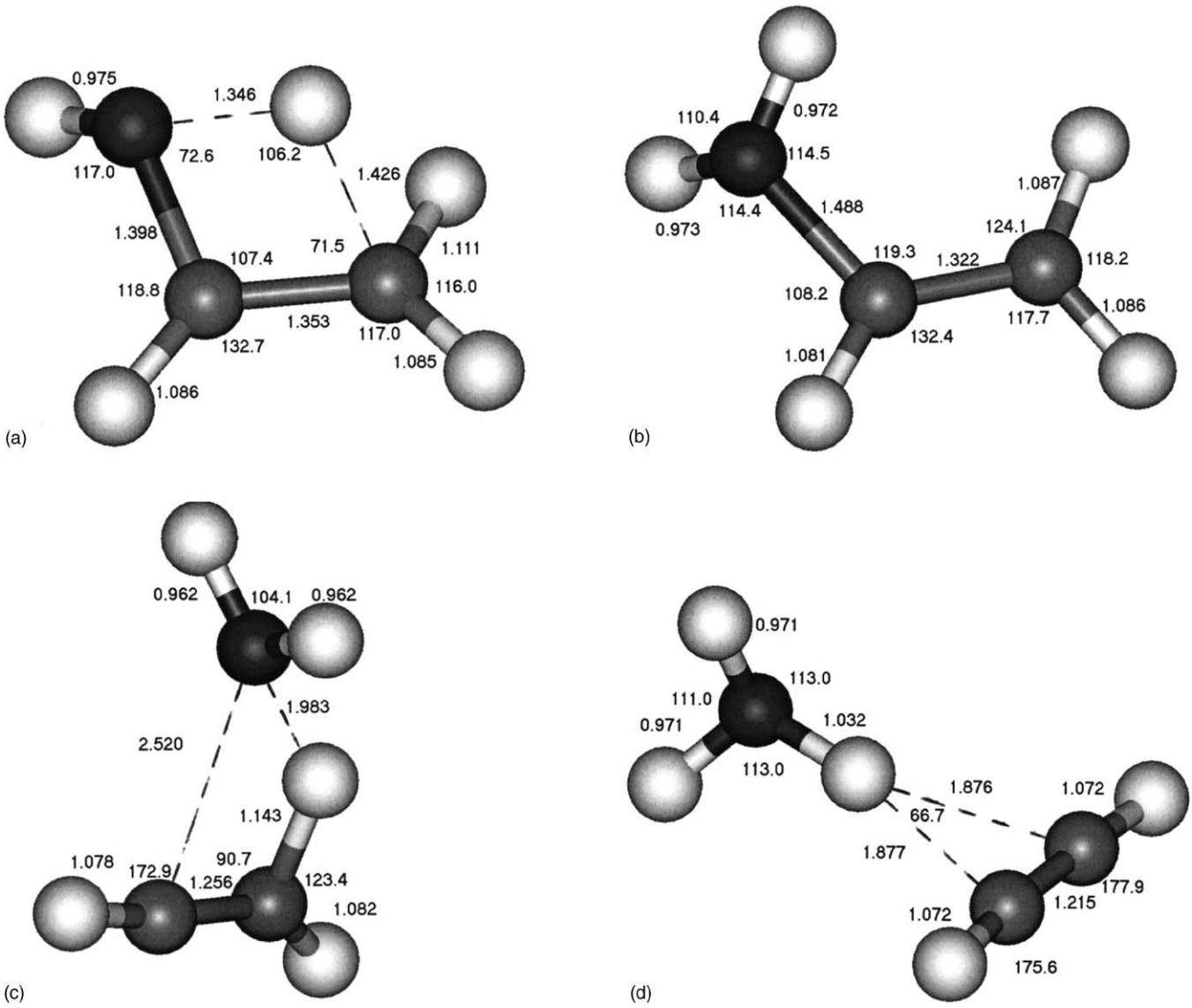

Fig. 3. (a) Geometry of the transition state for **1**t → $CH_2 = CHOH_2^+$ (**3**); (b) geometry of **3**; (c) geometry of TS(**3**) → $[HC{\equiv}CH \cdots H \cdots OH_2]^+$ (**4**); (d) geometry of **4**.

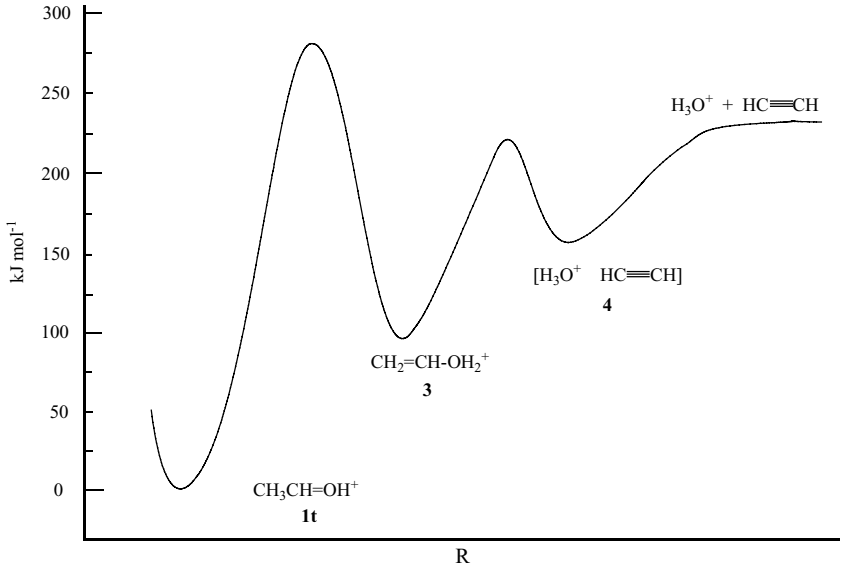

Fig. 4. Potential energy diagram for the pathway $CH_3CH{=}OH^+ \rightarrow H_3O^+ + HCCH$.

the pathway is given in Fig. 4. We found here that the reaction is initiated by transfer of a methyl H to the oxygen to form protonated vinyl alcohol, $CH_2{=}C(H){-}OH_2^+$ (**3**), a stable species connected to **1** by a transition state (Fig 3a). This species was previously identified as being stable by Radom and coworkers [8]. In **3**, all atoms except the two hydrogens on the oxygen are in a plane with the latter being symmetric on opposite sides of that plane (Fig. 3b).

In the second step, **3** → **4**, H_2O swings outward to above the center of the CC bond while a methylene H from the opposite end simultaneously swings over that center but much closer to the CC axis (Fig. 3c). This places H between the O and HC≡CH, forming H_3O^+ that is H-bonded to the acetylene triple bond in an ($H_3O^+ \cdots HC{\equiv}CH$) complex (**4**, Fig. 3d). This complex is a stable species with a binding energy of about 73 kJ mol^{-1} (Table 1). The geometry of TS(**3** → **4**) is given in Fig. 3c and changes in bond angles and distances to the itinerant species over the course of the reaction are plotted in Fig. 5. In this reaction O moves outward as it revolves. Revolution of H follows that of O and lengthening of the CH bond occurs last of all. Dissociation is assumed to occur from **4**; the energy for this would be supplied by TS(**1** → **3**) being at a higher energy than needed to dissociate **4** (Fig. 4). The formation of **4** is novel, although shift of an H to a bridging position generally accompanies formation of intermediate complexes containing $C_2H_5^+$, sometimes with the other partner moving to the outside of the bridging hydrogen [20–22]. These shifts are driven by the greater stability of the bridged $C_2H_5^+$ ion than of its classical form.

3.3. $CH_3O^+{=}CH_2 \rightarrow HCO^+ + CH_4$

The geometries of the ground and transition state for **2** → $HCO^+ + CH_4$ are given in Fig. 6. In the ground state of **2**, the methylene hydrogens are in the skeletal plane, and the methyl is bisected by this plane with one methyl hydrogen (H_s) in that plane cis to the CO bond. Methane elimination from $CH_3O^+{=}CH_2$ to generate HCO^+ is initiated by CH_3–O bond stretching (a minor amount of HOC^+ is also produced [3]). The methyl rotates H_s toward the oxygen as the CO bond lengthens. The CH_sO angle equals 172.9° at the IRC transition state and 180.0° at a short distance toward the products from the transition state. The H_sOC angle equals 92.7° at the transition state and does not change very dramatically throughout the reaction (from 97.7° at **2** to 87.8° and then to 99.5° on the way to the transition state and back to 86.1° near the separation of the products, i.e., the methyl swings around H_s during the reaction. Beyond the transition state, continued rotation brings the methyl C to where it can abstract the cis H from CH_2. The remainder of the reaction is energetically downhill, guiding the methane elimination to completion. The methyl swing causes H_t to be abstracted by the side of the methyl carbon opposite to that to which oxygen had been bonded. We attribute the swing around H_s to H_s being held in a confined area by attraction to the oxygen.

Audier et al. [3] obtained a transition state similar to ours, although their CH_sO angle was more bent than the one we found, and their $C_{Me}H_t$ bond was slightly longer (2.837 Å versus 2.493 Å). (Audier et al. used HF/6-31G(d) theory; our values are from QCISD/6-31G(d,p) theory). They did not trace the reaction coordinate, and so did not establish whether the methyl rolls over in their pathway. Methyl also turns over in the interconversion of $CH_3CH_2CHCH{=}OH^+$ and $CH_2{=}CHCH(CH_3)OH^{+\bullet}$) [23], so such somersaulting may not be unusual in methyl shifts.

In the vicinity of the transition state there is no covalent bonding between the methyl carbon and the oxygen, as the overlap population between those atoms is negative (−0.06

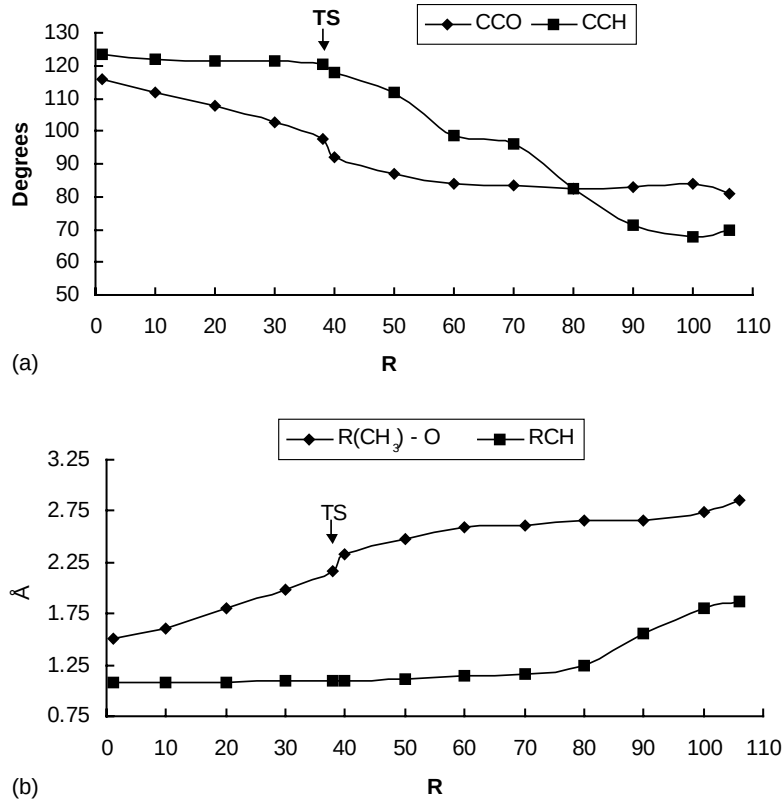

Fig. 5. Changes in the CCO and CCH angles (a) and CO and CH distances (b) during the conversion of $H_2C{=}CHOH_2^+$ to $[HC{\equiv}CH\cdots H\cdots OH_2]^+$. The CCH angle changes sooner than the CH distance, indicating that the H revolves around the C and then moves away from it. The *X*-axis values are numbers of steps the computation has taken along the reaction coordinate, a combination of geometric parameters of the system.

to −0.10) according to four different levels of theory. There is some covalent interaction between H_s and O, as that overlap population is positive (0.12–0.20; overlap for a normal CH bond is 0.7–0.8). The lack of covalent bonding between the O and C together with the temporal separation of bond cleavage and H-transfer clearly demonstrate that this reaction as ion–neutral complex-mediated. Furthermore, the rotation of the methyl during the course of the reaction neatly satisfies the "Reorientation Criterion" of Morton for identifying an ion–neutral complex; this criterion states that a complex exists when one of the partners is able to rotate around an axis perpendicular to a line between the partners [24]. Thus, present results verify the supposition of Audier et al. [3] that the reaction passes through a complex.

The very different mechanisms for methane elimination from **1** versus **2** provides insight into when an elimination reaction from a cation in the gas phase will go through a hypervalent intermediate rather than an ion–neutral complex, the latter occurring in most 1,2-eliminations from ions in the gas phase [25]. In methane elimination from **2**, cleavage of the CH_3–O bond is the lowest energy reaction available to **2**, so reaction proceeds by cleavage to form a complex. However, cleavage of the C–C bond in **1** would require much more energy, enough that H-transfer to form a hypervalent species becomes a lower energy process than C–C cleavage, and therefore occurs [4].

3.4. $CH_3O^+{=}CH_2 \rightarrow CH_2{=}O^+CH_3$

Reaction **2** → **2′** is facile at the dissociation threshold, as demonstrated by randomization of isotopically labeled carbons and hydrogens in the metastable decomposition of **2** [3]. Our goal was to establish whether **2** → **2′** is antarafacial (H_t moves from one side of the skeletal plane to the other in the course of the reaction), as in the homologous reaction $CH_3CH{=}O^+CH_3 \rightarrow CH_3CH_2O^+{=}CH_2$, or whether methylene rotates to perpendicular to the skeletal plane followed by H_t migration with H_t never leaving that plane. Enol → keto 1,3-H-shifts in radical cations, such as $CH_2CHOH^+ \rightarrow CH_3CHO^+$, take the latter type of pathway [6]. Previous work established that near the halfway point the planes of both CH_2 moieties are perpendicular to the skeletal plane in **2** → **2′** [8,9], but whether H_t leaves the skeletal plane or remains in it while approaching and departing from this point was not established.

Different levels of theory previously gave different results as to whether the halfway point in **2** → **2′** is an intermediate or a transition state [8,9]. In an effort to get consistent results, we characterized the TS(**2** → **2′**) by higher levels of theory than previously applied and by IRC calculations. The geometry of the transition state for **2** → **2′** is given in Fig. 7. We located only a transition state by B3LYP levels of theory. However, QCISD and QCISD(T) treatments

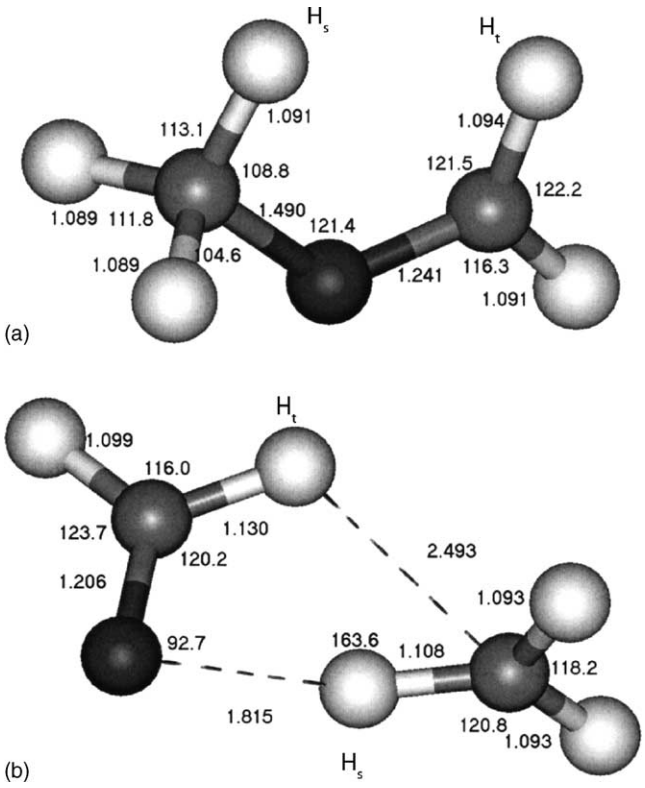

Fig. 6. (a) Geometry of $CH_3O^+{=}CH_2$ (**2**); (b) geometry of the transition state for abstraction of a hydrogen from CH_2O by CH_3 in the elimination of methane. The side abstracting the H is opposite to the side to which CH_2O was originally bonded.

gave all positive frequencies, classifying the halfway point as an intermediate. However, nearby energy maxima were only 0.076, 0.045 and 0.194 kJ mol^{-1} higher than the transition states (QCISD/6-31G(d), QCISD(T)/6-31G(d) and QCISD(T)/6-311G(2d,2p)//QCISD(T)/6-31G(d) theories, respectively), and zero point energy corrections made the symmetric point the highest energy point at all levels of theory. Therefore, we conclude that there is only a transition state near the symmetric, halfway point in **2** → **2′**.

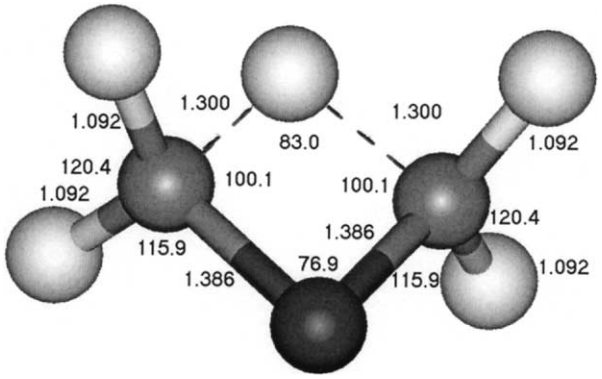

Fig. 7. Transition state for $CH_3O^+{=}CH_2$(**2**) → $CH_2{=}O^+CH_3$(**2′**).

In this study, IRC tracing demonstrated that, as in 1,3-H-transfers in enolic radical cations ([6], Hudson and McAdoo, unpublished), in **2** → **2′** the methylene rotates from being in the skeletal plane to being perpendicular to it before H-transfer begins, and the newly formed methylene rotates back into the plane after H-transfer ends (Fig. 8). Thus, π-bonding is essentially broken off before H-transfer commences. In contrast to $CH_3CH{=}O^+CH_3$ → $CH_3CH_2O^+{=}CH_2$, but as in enol → keto isomerizations of radical cations by 1,3-shifts, H-transfer occurs with H_t moving in the skeletal plane throughout the reaction. Thus, this is another 1,3-shift that is neither suprafacial nor antarafacial, but at the boundary between the two. Presumably the reaction evades the barrier imposed on a suprafacial pathway by the conservation of orbital symmetry while at the same time minimizing the strain that would be involved in an antarafacial transition state. Its demonstration in a closed shell system strengthens the hypothesis [6,7] that conservation of orbital symmetry is a factor causing radical cations to take this pathway, opposing doubts that conser-

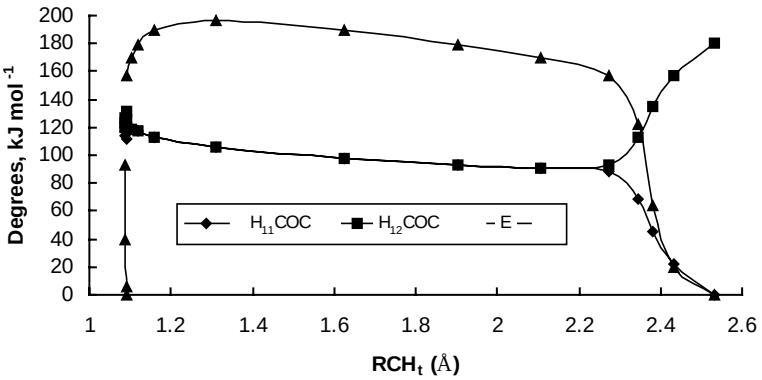

Fig. 8. Plots of the changes in the HCOC dihedral angles as a function of increasing CH_t distance during H-transfer from methyl to methylene in **2** → **2′** and of the system energy over the course of that reaction. Degrees and kJ mol^{-1} have coincidental numerical values on the *Y*-axis. Note that the methylene hydrogens are symmetric to the skeletal plane over much of the H-transfer, and that rotation of CH_2 takes place at the very end (beginning if reaction in the opposite direction is considered) of H-transfer. Also note that most of the required energy goes into CH_2 rotation (left side of the plots), and that once CH_2 is perpendicular to the skeletal plane, little additional energy is required by the H-transfer.

vation of orbital symmetry influences reactions of radical cations.

Nearly all of the energy expended in reaching the transition state is used to twist the methylene; once this geometry is attained, H-transfer requires very little additional energy (Fig. 8). However, in 1,3-shifts in enol radical cations comparable portions of the critical energy are needed to twist the methylene and then to transfer the hydrogen (Hudson and McAdoo, unpublished results). This difference is undoubtedly due to more energy being required to twist a π-bond containing two versus only one electron.

Detailed characterization of reaction coordinates in this work revealed informative features of reactions of $C_2H_5O^+$ isomers. The first three reaction characterized went through stages in which noncovalent bonding, either involving hypervalent entities or hydrogen bonding, was important. The last reaction demonstrates that orbital symmetry restraints can be avoided in closed shell species by taking a pathway along the boundary between being suprafacial and antarafacial. Future tracing of reaction coordinates will undoubtedly add further to our understanding of gas phase ion chemistry.

Acknowledgements

We thank Debbie Pavlu and Bhavin Shah for assistance with manuscript preparation.

References

[1] T.W. Shannon, F.W. McLafferty, J. Am. Chem. Soc. 88 (1966) 5021.
[2] B.G. Keyes, A.G. Harrison, Org. Mass Spectrom. 9 (1974) 221.
[3] H.E. Audier, G. Bouchoux, T.B. McMahon, A. Milliet, T. Vulpius, Org. Mass Spectrom. 29 (1994) 176.
[4] C.E. Hudson, L. DeLeon, D. Van Alstyne, D.J. McAdoo, J. Am. Soc. Mass Spectrom. 5 (1994) 1102.
[5] R.B. Woodward, R. Hoffmann, Angew. Chem. 8 (1967) 781.
[6] C.E. Hudson, D.J. McAdoo, Int. J. Mass Spectrom. 219 (2002) 295.
[7] C.E. Hudson, D.J. McAdoo, J. Org. Chem. 68 (2003) 2735.
[8] R.H. Nobes, W.R. Rodwell, W.J. Bouma, L. Radom, J. Am. Chem. Soc. 103 (1981) 1913.
[9] C.E. Hudson, D.J. McAdoo, J. Am. Soc. Mass Spectrom. 9 (1998) 130.
[10] M.J. Frisch, G.W. Trucks, H.B. Schlegel, G.E. Scuseria, M.A. Robb, J.R. Cheeseman, V.G. Zakrzewski, J.A. Montgomery, Jr., R.E. Stratmann, J.C. Burant, S. Dapprich, J.M. Millam, A.D. Daniels, K.N. Kudin, M.C. Strain, O. Farkus, J. Tomasi, V. Barone, M. Cossi, R. Cammi, B. Mennucci, C. Pomelli, C. Adamo, S. Clifford, J. Ochterski, G.A. Petersson, P.Y. Ayala, Q. Cui, K. Morokuma, D.K. Malick, A.D. Rabuck, K. Raghavachari, J.B. Foresman, J. Cioslowski, J.V. Ortiz, A.G. Baboul, B.B. Stefanov, G. Liu, A. Liashenko, P. Piskorz, I. Komaromi, R. Gomperts, R.L. Martin, D.J. Fox, T. Keith, M.A. Al-Laham, C.Y. Peng, A. Nanayakkara, M. Challacombe, P.M.W. Gill, B. Johnson, W.Chen, M.W. Wong, J.L. Andres, C. Gonzalez, M. Head-Gordon, E.S. Replogle, J.A. Pople, Gaussian, Inc., Pittsburgh, PA, 1998.
[11] C. Gonzalez, H.B. Schlegel, J. Chem. Phys. 90 (1989) 2154.
[12] C. Gonzalez, H.B. Schlegel, J. Phys. Chem. 94 (1990) 5523.
[13] A.P. Scott, L. Radom, J. Phys. Chem. 100 (1996) 16502.
[14] W.J. Hehre, L. Radom, P.V.R. Schleyer, J.A. Pople, Ab Initio Molecular Orbital Theory, John Wiley and Sons, New York, 1986, p. 145.
[15] A.J.R. Heck, L.J. de Koning, N.M.M. Nibbering, J. Am. Soc. Mass Spectrom. 2 (1991) 453.
[16] E.T. White, J. Tang, T. Oka, Science 284 (1999) 135.
[17] C.E. Hudson, S. Eapen, D.J. McAdoo, Int. J. Mass Spectrom. 228 (2003) 955.
[18] E. Uggerud, Mass Spectrom. Rev. 18 (1999) 285.
[19] C.E. Hudson, D.J. McAdoo, Int. J. Mass Spectrom. 214 (2002) 315.
[20] G. Bouchoux, F. Penaud-Berruyer, H.E. Audier, P. Mourgues, J. Tortajada, J. Mass Spectrom. 32 (1997) 188.
[21] C.E. Hudson, D.J. McAdoo, J. Am. Soc. Mass Spectrom. 9 (1998) 138.
[22] S. Olivella, A. Solé, D.J. McAdoo, J. Am. Chem. Soc. 118 (1996) 9368.
[23] C.E. Hudson, D.J. McAdoo, Int. J. Mass Spectrom. 199 (2000) 41.
[24] T.H. Morton, Org. Mass Spectrom. 27 (1992) 353.
[25] D.J. McAdoo, R.D. Bowen, Eur. Mass Spectrom. 6 (1999) 389.